energies

MDPI

Article

Evaluation of Physicochemical Properties Composite Biodiesel from Waste Cooking Oil and *Schleichera oleosa* Oil

Suherman Suherman [1,2], Ilmi Abdullah [1,*], Muhammad Sabri [1] and Arridina Susan Silitonga [3,4]

[1] Department of Mechanical Engineering, Universitas Sumatera Utara, Medan 20155, Indonesia; suherman@umsu.ac.id (S.S.); m.sabri@usu.ac.id (M.S.)
[2] Department of Mechanical Engineering, Universitas Muhammadiyah Sumatera Utara, Medan 20238, Indonesia
[3] Department of Mechanical Engineering, Politeknik Negeri Medan, Medan 20155, Indonesia; arridina@polmed.ac.id
[4] Center for Technology in Water and Wastewater, School of Civil and Environmental Engineering, Faculty of Engineering and Information Technology, University of Technology Sydney, Sydney, NSW 2007, Australia
* Correspondence: ilmi@usu.ac.id

Abstract: Waste cooking oil (WCO) biodiesel has some disadvantages, such as poor cold flow properties, low oxidation stability, and flash point during storage. These poor physicochemical properties can be improved by different ways, such as the addition of non-edible oil. The aim of this study to analyse physicochemical properties of the biodiesel made by between WCO and *Schleichera oleosa* (SO). The biodiesel produced with 70:30% of WCO and SO respectively as crude oil, further introducing of different KOH-based catalyst into this oil to obtained the methyl ester. The optimum yield transesterification process are 94% with 60 min. of the reaction time, 1 wt.% KOH, and 12:1 molar ratio the methanol to oil. On the other hand, the *Schleichera oleosa* blend shows oxidation stability at 6.8 h and 3.3 h for Waste cooking oil methyl ester (WCME). The reduction of cold flow and, on the contrary, the flash point increase were obtained with a 70:30% ratio of WCO and SO. The cold flow properties and flash point of the fuel. Thus, mixed WCO and *Schleichera oleosa* oil improve the physiochemical properties such as oxidation stability, flash point, and cold flow of biodiesel without the need for synthetic antioxidants.

Keywords: biodiesel; cold flow; oxidation stability; waste cooking oil

Citation: Suherman, S.; Abdullah, I.; Sabri, M.; Silitonga, A.S. Evaluation of Physicochemical Properties Composite Biodiesel from Waste Cooking Oil and *Schleichera oleosa* Oil. *Energies* **2023**, *16*, 5771. https://doi.org/10.3390/en16155771

Academic Editor: Attilio Converti

Received: 3 May 2023
Revised: 9 June 2023
Accepted: 23 June 2023
Published: 2 August 2023

1. Introduction

The increase in energy consumption is driven by the rapid growth of the manufacturing and transportation industries [1]. However, this increased consumption has also raised concerns about the depletion of non-renewable energy sources, such as coal, oil, and gas, and the sustainability of current energy practices [2]. To address these challenges, there is a need for a concerted effort toward transitioning to renewable energy sources and improving energy efficiency. The post-COVID-19 era is expected to see a rise in industrial fuel consumption [1], with the transportation sector accounting for about 25% of global energy consumption [3]. Diesel engines are widely used in various industries, including transportation, agriculture, manufacturing, and construction, due to their high performance and reliability [4]. However, diesel engines also emit harmful gases that cause environmental pollution [5]. The high consumption of fossil fuels not only contributes to the depletion of fuel reserves but also causes environmental problems such as acid rain, air pollution, climate change, and worsened drought conditions [6]. Therefore, diesel engines should adopt environmentally friendly fuels to address the oil crisis and environmental pollution [4]. Biodiesel, a non-petroleum-based alternative fuel, is one such source of renewable energy [7]. It produces less carbon monoxide, hydrocarbons, and certain materials but produces higher nitrogen oxide (NOx) emissions [8]. Biodiesel also has a higher flash

point and lubricity than diesel [9]. Due to the high cylinder temperature in diesel engines, fast combustion can lead to higher NOx production [10].

Biodiesel can be produced from a wide range of oils, including both edible and non-edible varieties, as well as waste oils and animal fats [11]. Biodiesel can be classified into three generations: the first generation, which is derived from edible vegetable oils such as palm oil [12], coconut oil [13,14], sunflower oil [15], and soybean oil [16,17]; as well as non-edible oils such as Calophyllum inophyllum [18,19], jatropha curcas oil [19], Reutealis trisperma [20], Ceiba pentandra [21], mustard oil [22], beauty leaf oil [23], rubber seed oil [24], and mahua oil, in addition to animal fats [25]. The second generation includes biodiesel from waste cooking oil [7,26]. Nowadays, various studies worldwide are investigating biodiesel production from microalgae, which is considered the third generation [27,28].

Biodiesel can be produced from waste cooking oil (WCO) through a transesterification process that uses an alkali, acid, or enzyme catalyst [29]. Generally, the transesterification process uses homogeneous catalysts [30]. This type of catalyst has the advantages of a short reaction time (1 h) and high availability [31]. Several studies conducted on synthetic biodiesel used heterogeneous [32] and enzymatic catalysts [33–35]. However, the high free fatty acid content (FFA) in WCO causes saponification [36]. In addition to developing many new catalysts in biodiesel production, production techniques such as using infrared [37], microwave [7,38], ultrasound [33], electromagnetic [34], and solar parabolic [39] in the synthesis of WCO biodiesel were also developed.

The quality of fuel significantly impacts the oxidation stability level during the storage of biodiesel produced from WCO [40]. However, biodiesel derived from WCO has disadvantages, such as poor oxidation stability and cold flow properties [23]. The water content of WCO is higher than that of fresh oil due to the frying operation. As a result, this can lead to an increase in free fatty acids, which can cause saponification, ultimately resulting in a reduction in the yield of biodiesel [38].

The type of catalyst used in the transesterification process can impact the resulting biodiesel's cold flow properties and oxidation stability. For instance, the use of heterogeneous catalyst CaO-Al_2O_3 has resulted in lower cold flow properties than when KOH is used. However, CaO-Al_2O_3 was found to produce biodiesel with higher oxidation stability compared to those produced using potassium hydroxide (KOH) [30]. Furthermore, Wang. et al. [41] reported that biodiesel viscosity and low-temperature flow properties increased with polymethyl acrylate (PMA).

Biodiesel tends to deteriorate in quality over time due to its susceptibility to oxidation [42]. An oxidation stability test is used to predict the shelf life of biodiesel [30]. During the process of deterioration, secondary complex reactions occur, leading to the formation of hydrogen peroxide and an increase in the acid value [43]. This process also causes the formation of compounds and undesirable changes in properties [40]. Additionally, oxidation can negatively impact the chemical and physical properties of the fuel, resulting in the formation of insoluble gums that can clog fuel filters [44]. As a result, biodiesel that has undergone oxidation is unsuitable for use [42]. Oxidised biodiesel can also pose problems in cold climates [45]. Unfortunately, biodiesel's poor cold flow properties and oxidation stability are its primary quality determinants. Factors such as light and temperature can affect biodiesel oxidation stability [40]. The degradation time of the fuel is significantly influenced by contaminants, storage container characteristics, fatty acid profile, and the absence of antioxidants [46]. Despite its poor oxidation stability, biodiesel has the advantage of high lubricity, which can increase brake power and reduce friction losses. Furthermore, biodiesel has a high cetane and oxygen content but produces low sulfur emissions [9].

Fatty acid methyl ester fuel, when stored for extended periods, can form carbon deposits. This, in turn, can cause operational issues within the fuel system and blockages in diesel engine fuel filters [32,47]. According to Bezergianni et al. [48], after 12 months of storage, water content, viscosity, total acid number, and density increased in WCO biodiesel. The resulting polymer is insoluble in diesel fuel, limiting fuel injection and pumping [40].

Furthermore, this polymer can cause corrosion within the fuel injection system and increase wear due to aldehydes and short-chain acids forming in biodiesel [40].

Recently, many studies have been conducted to improve the low-temperature operation of biodiesel, including adding additives [49], antioxidants [50], modifying structures [51], and biodiesel–diesel blending [52]. Blending different feedstocks can enhance biodiesel properties. Several studies have also been conducted on WCO biodiesel and other oil blends. Milano et al. [7] reported that a mixture of biodiesel WCO and *Calophyllum inopylum* (70:30) reduced the wear scar diameter (WSD) in lubricated ball bearings. In another study, Milano et al. [23] explored different oils, including beauty leaf oil, Calophyllum inophyllum, *Jatropha curcas*, and WCO (30:70), to increase the oxidation stability of WCO biodiesel. They concluded that applying WCO biodiesel and *Calophyllum inophyllum* (70:30) effectively enhanced the oxidation stability. Furthermore, the biodiesel blends *Calophyllum inophyllum-Ceiba pentandra* (60:40) fulfill ASTM D6751 [53]. Dharma et al. [54] found that the biodiesel blend of *Jatropha curcas-Ceiba Pentandra* (J50C50) reduced smoke opacity and carbon dioxide emissions. Biodiesel B10 showed engine performance similar to diesel fuel in brake power, thermal brake efficiency, and engine torque. Moreover, Milano et al. [23] obtained that WCO biodiesel has high oxidation stability within 22 h. Blending *Canola* oil with WCO and mixed biodiesel improved cold flow properties, besides oxidation stability and fire point upon extended storage [55].

Furthermore, the physicochemical and cold flow properties of WCO biodiesel can improve with added natural and synthetic antioxidants. A study by Zhang et al. [56] demonstrated that adding polymethacrylate (PMA) to soybean biodiesel led to a 17 h increase in oxidation stability with only 2000 ppm. However, the use of Tert-Butyl-Hydroquinone (TBHQ) as a synthetic antioxidant was found to be the most effective, with an induction period (IP) of 10.19 h, although it did result in increased exhaust emissions (CO, NOx, and HC) [47]. Jain and Sharma [57] discovered that the addition of pyrogallol (PY) was more efficient in metal-contaminated *Jatropha curcas* biodiesel as compared to other additives, such as TBHQ, butylated hydroxytoluene (BHT), propyl gallate (PG), and butylated hydroxyanisole (BHA). Meanwhile, there was a slight increase in the acid value, viscosity, and moisture content of the stored sample, whereas there was a slight decrease in the iodine number. However, it is important to note that the storage of WCO biodiesel for over a year exceeds the appropriate standard [40].

Adding antioxidant doping to biodiesel enhances its oxidation stability when exposed to air, light, and metals [8]. The presence of metal ions, such as Copper (Cu), Iron (Fe), Manganese (Mn), and Carbon Monoxide (CO) in biodiesel can increase the oxidation rate even at low concentrations [46]. Biodiesel with a high content of oleic and palmitic acids tends to have greater oxidation stability [58]. According to Barti and Singh [42], the addition of 1000 ppm (*Camellia assamica*) extract as an antioxidant increased the WCO biodiesel induction period by 146% (from 2.88 h to 4.11 h) [42]. Serquera et al. [59] stated that additional antioxidants such as curcumin, propyl gallate, butyl-hydroxyanisole, and tert-butyl hydroquinone slow down biodiesel degradation and corrosion rate on metals (carbon steel and copper). Cold flow properties are also crucial in biodiesel, particularly in areas with cold weather [30]. The operation of biodiesel at low temperatures causes the crystallisation of saturated fatty acid esters, which can block the fuel filter [52]. Different natural and synthetic antioxidants used to improve the cold flow and oxidation stability of WCO biodiesel are shown in Table 1.

Numerous studies have investigated biodiesel production from WCO, examining the impact of using different feedstocks on the resulting methyl ester yield and properties. Despite several articles on WCO biodiesel production being available in the literature, only a few focus on producing WCO biodiesel blended with other feedstocks. Additionally, there is no study on biodiesel production using a mixture of WCO and *Schleichera oleosa*. This study aimed to improve the pour point, flash point, and oxidation properties of biodiesel produced from WCO by mixing it with *Schleichera oleosa* oil. It will examine the potential raw materials for blending biodiesel from WCO and *Schleichera oleosa*, characterise

the physicochemical properties of the biodiesel produced, and evaluate the influence of the catalyst amount on kinematic viscosity and density. Finally, the production time and the impact of the oil molar ratio on the methyl ester yield will also be discussed. By blending *Schleichera oleosa* oil into WCO, biodiesel physiochemical properties are expected to improve.

Table 1. Literature of the added natural and synthetic antioxidants for improvement of cold flow and oxidation stability of WCO Methyl ester.

Type of Biodiesel	Improver	Loading	Cold Flow			Oxidation Stability (h)	Ref.
			CP (°C)	PP (°C)	CFPP (°C)		
WCO	Polymethyl acrylate (PMA)	0.04%	−9	−17	−11	-	Wang [41]
WCO	WCO-Calophyllum inophyllum	70:30	4	3	4	18.14	Milano [7]
WCO	Green tea	1000 ppm	-	-	-	2.88	Bharti [42]
WCO	Canola	Mixed oil (65:35)	9	1.7	-	9.25	Kassem [55]
WCO	Pyrogallol (PY)	750 ppm	9	11	3	-	Uguz [60]
WCO	TBHQ	1000 ppm	-	-	-	51.2	Zhou [55]
WCO	Thuja oreantalis L.	100 ppm	-	-	-	6.79	Devi [61]
WCO	ethylene-vinyl acetate (EVA)	0.1%	5	10	11	25.56	Sun [62]

2. Materials and Methods

2.1. Materials

Waste cooking oil (WCO) was collected from cafes in Medan City, North Sumatra, and crude *Schleichera oleosa* (SO) oil was obtained from Probolinggo, East Java, Indonesia. The experiment employed several chemicals, including 99.9% pure methanol (ACS reagent grade), >98.9% pure H_2SO_4, H_3PO_4, filter paper (110 mm in diameter), and 99% pure KOH pellets. Table 2 lists the physiochemical properties of *Schleichera oleosa* oil, WCO, and WCOK30 crude oil. Physiochemical properties include density at 40 °C, dynamic viscosity at 40 °C, kinematic viscosity at 40 °C, calorific value, oxidation stability, and acid value.

Table 2. Properties of crude oil WCO, SO, and WCOK30.

Property	Unit	Crude Oils				Crude Oil Mixtures	
		WCO [a]	WCO [23]	SO [b]	Kusum [63]	WCOK30 [c]	WC70JC30 [23]
Kinematic viscosity at 40 °C	mm^2/s	41.65	49.05	40.48	40.36	41.21	47.09
Dynamic viscosity at 40 °C	mPa s	37.65	44.27	36.36	-	37.05	42.52
Density at 40 °C	kg/m^3	916	902.70	915	860	916	902.90
Acid value	mg KOH/g	3.92	2.19	18	-	10	13.26
Higher heating value	MJ/kg	39.561	38.59	39.462	38.5	39.676	38.03
Oxidation stability 110 °C	H	3.5	3.6	9.3	-	7	1.38

[a,b,c] Result; WCME = waste cooking methyl ester; UCME = used cooking oil methyl ester; KOME = *Schleichera oleosa* methyl ester; KSME = Kusum oil methyl ester; WSME = waste cooking and *Schleichera oleosa* methyl ester and mixed (70:30); W70CI30 = waste cooking oil and *Calophyllum inopyllum* (70:30).

2.2. Equipment Set Up

The degumming and ester/transesterification processes were conducted by using the equipment setup shown in Figure 1. These processes were carried out in a 1 L double jacket reactor fitted with an overhead stirrer (model IKA RW 20). The reactor was also equipped with a circulating water bath heater (DSC 1000 model) with a timer and a 2 L

temperature capacity. The glass condenser was connected to a water cooling bath with a pump circulating 0.05 L/s of water.

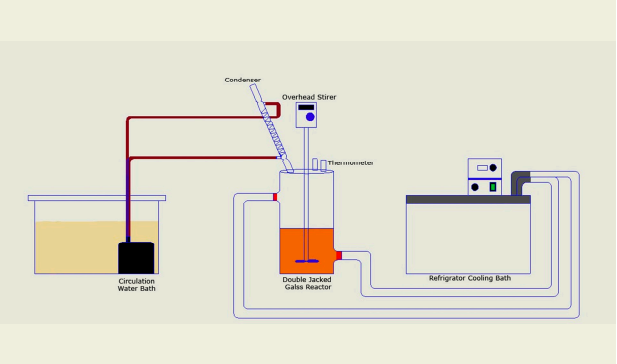

Figure 1. Experimental setup for ester and transesterification.

2.3. Biodiesel Production

The WCO was first filtered to eliminate any impurities and then heated to remove any remaining water content., The WCO was subsequently mixed with *Schleichera oleosa* oil at a volume ratio of 70:30 to create a blend known as WCOK30. However, upon analysis, it was found that the free fatty acid (FFA) content in the waste cooking oil and *Calophyllum inopyllum* (70:30) (WCOK30) crude oil exceeded the acceptable limit of 3.92% (2%). Furthermore, the degumming process must be carried out to reduce FFA and gum in WCOK30 crude oil by heating in a double jacket reactor with a 1 L capacity set at 60 °C. A 20% concentration of H_3PO_4 (at a volume of 2%) was added to the blend and continuously agitated for 30 min at a rotation speed of 800 rpm, as depicted in Figure 1.

After the degumming process, esterification was carried out by blending the degummed oil with methanol in a molar ratio of 10:1, along with 2% (v/v) sulfuric acid (H_2SO_4). The esterification reaction occurred in a 1 L double-jacketed reactor set at a temperature of 60 °C, with a stirring speed of 1000 rpm for 1–2 h. Following the completion of the reaction, the oil and methanol were separated using a separatory funnel. Upon observation, it was noted that the contents of the separatory funnel separated into two distinct layers, with the esterified oil settling in the bottom layer and the methanol in the top layer. The esterified oil was then collected for further processing through transesterification. The Flow chart of esterification and transesterification from WCO, SO and WCOK30 are shown in Figure 2.

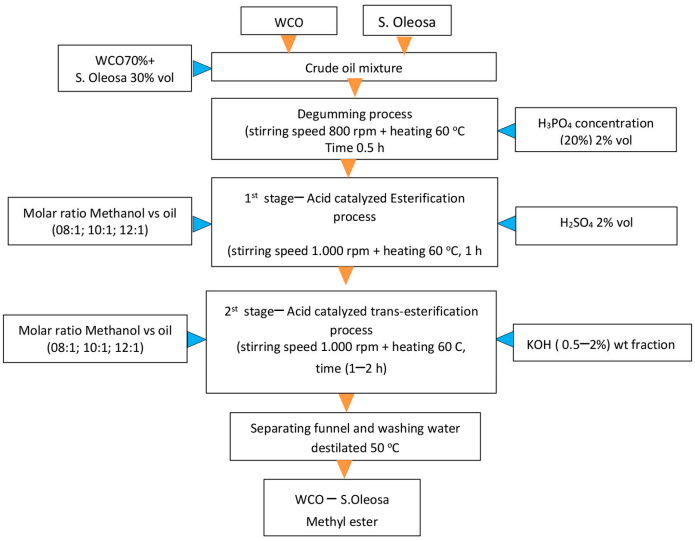

Figure 2. Flowchart esterification and transesterification process of WCME, KOME and WSME.

Transesterification was conducted to esterify the oil by adding a volume percentage of sodium hydroxide (KOH) (0.5–2%) which was dissolved in methanol in molar ratios of 8:1, 10:1, and 12:1. The mixture was stirred at 1000 rpm for 1–2 h at a temperature of 60 °C. The resulting mixture was separated into two layers, with crude biodiesel on top and methanol on the bottom, by using a separatory funnel. The biodiesel was further washed with distilled water at 50 °C to remove methanol and glycerol. The residual water and methanol were eliminated by heating the WCOK30 biodiesel in a rotary evaporator at 90 °C, followed by filtration with filter paper.

2.4. Analysis of Crude Oil and Biodiesel

The physical and chemical properties of crude oil and biodiesel were analysed, including high heating value, acid value, kinematic viscosity at 40 °C, density at 15 °C, and oxidation stability at 110 °C. Additionally, pour point, flash point, cloud point, copper strip corrosion, sulfur content concentration, and carbon residue were also characterised. The equipment used to analyse the physicochemical properties of both crude oil and biodiesel is listed in Table 3.

Table 3. Equipment and Test Methods for physicochemical properties.

Property	Equipment	Standard Method
Kinematic viscosity at 40 °C	SVM 3000 viscometer cold properties (Anton Paar, Austria)	ASTM D455
Density at 15 °C	SVM 3000 viscometer cold properties (Anton Paar, Austria)	ASTM D455
Cloud and pour point	LAB 1300 ST Linetronic technologies, Switzerland	ASTM D2500
Heating value	Automatic calorimeter, IKA C2000, China	ASTM D4809
Acid number and iodine value	ECH 7000 Titrator Type TAN/TBN Titrator (ECH Germany)	ASTM D664
Flash point	PMA 5 Pensky Martens flash point tester (Anton Paar, Austria)	ASTM D93
Copper strip corrosion	KOEHLER k25339 Copper strip corrosion test tube bath	ASTM D130
Sulfur content	Sulfur Meter X-Ray Tanaka Scientific RX 360SH	ASTM D4294
Carbon residue	Koehler K80030 Condradson Carbon residue test	ASTM D189
Oxidation stability at 110 °C	rapidOxy 100 fuel (oxidation stability tester (Anton Paar, Germany	ASTM 7525
FAME content	Gas Chromatography system	EN 14103
DSC	DSC 214 Polyma NETZSCH	ASTM D3418
GC-MS	Shimadzu Type QP2010 Plus	ASTM6751
FTIR	Bruker ALFA II	ASTM E2412

2.5. DSC Measurement of WCME and WSME

The DSC type 214 (Polyma, NETZSCH) was used to measure the crystallisation initiation temperature and enthalpy of freezing during the phase transformation of waste cooking methyl ester (WCME) and waste cooking and *Schleichera oleosa* methyl ester and mixed (70:30) (WSME). A sample of 8 mL was placed into a mini aluminum pan, and the heat flow from the sample was compared to the reference temperature. The sample was heated and cooled over a temperature range of 20 °C to −80 °C, with a flow rate of 10 °C/min, under a Nitrogen (N_2) atmosphere. The equipment and test methods used for the physicochemical properties of crude oil and biodiesel are shown in Table 3.

3. Results and Discussion

3.1. Characterisation Properties of Crude Oil WCO, SO, and WCOK30

Table 2 contains information on the physical and chemical properties, such as kinematic and dynamic viscosities, acid and higher heating values, density, and oxidation stability.

The present study found that the kinematic viscosity and density of WCO were slightly lower as compared to the values reported by Milano et al. [23]. Specifically, the kinematic

viscosity is 41.65 mm^2/s, while the density is 916 kg/m^3, whereas Milano et al. reported values of 49.05 mm^2/s and 902.70 kg/m^3, respectively. On the other hand, the kinematic viscosity of *Schleichera oleosa* is slightly higher than that reported by Sharkar et al. [63], with a value of 40.48 mm^2/s as compared to 40.36 mm^2/s. Regarding the higher heating value, the study found that *Schleichera oleosa* had a slightly higher value (39.462 MJ/kg) than Sharkar et al. [63]. (38.5 MJ/kg).

In relation to *Schleichera oleosa* oil, the present study compared its physical properties with those reported in preliminary studies. The kinematic viscosity and density were 40.36 mm^2/s and 915 kg/m^3, respectively. The kinematic viscosity of *Schleichera oleosa* was similar to that reported by Sarkar et al. [63] (40.36 mm^2/s), but the viscosity was higher than what was reported. On the other hand, the high heating values of WCO, *Schleichera oleosa*, and WCOK30 were similar to the results reported in preliminary studies. The high heating value of crude oil *Schleichera oleosa* was observed to be higher (39.462 MJ/kg) as compared to the value reported by Sarkar et al. [63], at 38.5 MJ/kg.

In comparison to the results reported by other studies, the kinematic viscosity of WCOK30 was lower (41.21 mm^2/s) as compared to the value reported by Milano et al. [23] (47.09 mm^2/s). The density of WCOK30 was slightly higher at 916 kg/m^3 compared to 902 kg/m^3, as reported by Milano et al. [23], Consequently, the higher heating value and oxidation stability of WCOK30 differed from other mixed oil, as reported by Milano et al. [23], with values of 39.676 MJ/kg and 38.03 MJ/kg, respectively. The research found a significant difference in the oxidation stability of WCOK30 crude oil compared to the results reported in other studies. The oxidation stability of WCOK30 crude oil was higher at 7 h as compared to 1.38 h of WC70CI30 crude oil reported by Milano et al. [23].

3.2. Density and Kinematic Viscosity of WCME, KOME, and WSME

The density of biodiesel, as measured following the ASTM D1298 standard [9], is a critical factor that impacts the fuel injection process and combustion efficiency in diesel engines. The density of biodiesel plays a crucial role in fuel injection and atomisation, directly affecting the engine's thermal efficiency [64]. Typically, biodiesel density is higher than diesel fuel, leading to increased in injection time and spraying penetration [65]. In order to evaluate the physicochemical properties of WCO, SO, and WSME, the study measured several parameters, as shown in Table 4. The present study observed that the density of the WCME (875 kg/m^3) was marginally lower than *Schleichera oleosa* methyl ester (KOME) (879 kg/m^3). On the other hand, the density of WSME (857 kg/m^3) was higher than KOME and WCME.

It was found that at 40 °C, WSME had a kinematic viscosity of 4459 mm^2/s, slightly lower than WCME (4.498 mm^2/s) and KOME (4.472 mm^2/s). The kinematic viscosity of biodiesel WCME, KOME, and WSME at 40 °C was slightly higher than that of diesel fuel (2986 mm^2/s). The high kinematic viscosity of biodiesel can greatly impact the spray atomisation process, causing a reduction in the intake stroke and ignition delay in the mixing of fuel and air in the combustion chamber [9]. Biodiesel has a greater viscosity, which is 10 to 15 times higher than diesel because it has a larger atomic mass, and this tends to reduce thermal efficiency [64]. Higher kinematic viscosity can cause engine chamber deposits, while lower viscosity reduces engine lubrication [23]. The kinematic viscosity correlates with the acid value. Generally, fuel quality is assessed based on the measured increase in kinematic viscosity and acid values of samples because these parameters correlate with acid formation as oxidation progresses [8]. Despite a reduction in kinematic viscosity and density by 0.867% and 2.057%, respectively, the cloud points of WCME, KOME, and WSME tend to fulfill ASTM D6751 and EN 14214 standards.

3.3. Acid Value, the Concentration of Sulfur Residue, and Carbon Residue

The acid values of WCME, KOME, and WSME were 0.132 mg KOH/g, 0.308 mg KOH/g, and 0.28 mg KOH/g, respectively. The increase in acid value from 0.132 mg KOH/g to 0.308 mg KOH/g satisfies the range required by ASTM 6751 standard. The

addition of *Schleichera oleosa* into WCO led to a slight reduction in the sulfur residue of WSME from 0.092 (*w*/*w*)% to 0.0079 (*w*/*w*)%. Moreover, the carbon residues of WSME and KOME wereslightly higher than that of WCME, at 0.00015% and 0.00034%, respectively. The carbon residue of WSME was lower than the result reported by Milano et al. [23], at 0.03%.

3.4. Heating Value

The heating value is a crucial property of diesel engines used in heavy vehicles as it impacts fuel consumption and efficiency [66]. Table 4 shows the heating values of crude oil WCO, *Schleichera oleosa*, and WCOK30. The heating value of diesel oil is higher as compared to biodiesel. The calorific value of conventional diesel exhibits a high heating value of 46 MJ/kg, as shown in Table 4. In the current study, the high heating value of biodiesel derived from WCME, KOME, and WSME was 40.047 MJ/kg, 39.889 MJ/kg, and 39.952 MJ/kg, respectively. However, the high heating value of all biodiesel was slightly lower than that of WCO biodiesel [38]. As a result, the high heating value of biodiesel is usually lower than that of conventional diesel, leading to a slight reduction in engine power and torque of 7% and 8%, respectively [27]. The current results of biodiesel which has a high heating value (HHV) correspond with previous studies. Specifically, the HHV of the WSME (49.953 MJ/kg) was slightly lower in comparison with mixed WCO-Calophyllum inophyllum biodiesel at 40.82 MJ/kg, which was reported by Milano et al. [23]. Furthermore, the high oxygen content of biodiesel causes lower calorie values than diesel fuel (46.200 MJ/kg).

3.5. Temperature

Flash point (FP), pour point (PP), and cloud point (CP) are important parameters to consider when evaluating biodiesel. A high flash point is necessary to prevent fires during storage, handling, and transportation [67]. The volatility of the fuel is inversely related to its flash point, and the presence of solvents and residual alcohol in biodiesel can lower its flash point [9]. Low pour and cloud points are desirable for biodiesel to perform well in cold climates [38]. Table 4 shows the flash, pour, and cloud points of WCME, KOME, and WSME. However, WSME had the highest flash point, followed by *KOME* and WCME. The flash point of WSME was 172 °C, followed by KOME at 154 °C, and the lowest was WCME at 98 °C. This exceeds the limit of the ASTM D6751 standard. A high quantity of saturated (SFA) compounds can produce high pour and cloud points [46].

The current study demonstrated that blending WCO and *Schleichera oleosa* mixed oils can enhance certain characteristics of biodiesel, including its cold flow properties. A critical property affecting low-temperature operation is the pour point, which is lowered as the value decreases. In the present study, the WSME pour point decreased from 12 °C to 9 °C. As the fuel temperature drops, it can cause the formation of wax crystals, leading to the solidification of the oil and clogging of the injectors and fuel filters. The cloud point is the temperature at which the first visible wax crystals are observed in the fuel [9,66]. Table 4 shows the CPof WCME, KOME, and WSME. The addition of *Schleichera oleosa* to WCO at a ratio of 70:30 improved the CP of the biodiesel by 19%, with a decrease from 25 °C to 21 °C.

The PP and CP values of WCME, KOME, and WSME were higher as compared to those reported in previous studies, as shown in Table 4. The results obtained indicated that the PP values for WCME, KOME, and WSME were 12 °C, 9 °C, and 9 °C, respectively.

Table 4. Comparison of physicochemical properties of the WCME, KOME, and WSME produced.

Properties	Unit	Biodiesel ASTM D6751	Diesel	WCME [a]	Waste Cooking [68]	KOME [b]	Kusum Oil [69]	WSME [c]	W70CI30 [7]	Improve
Kinematic viscosity at 40 °C	mm^2/s	1.9–6.0	2.986	4.498	3.2	4.472	4.71	4.459	5.12	−0.867
Density at 40 °C	kg/m^3	880	823	875	876	879	875.6	857	878	−2.057
Acid value	mg KOH/g	0.5 (maks)	-	0.132	-	0.308	-	0.28	0.57	112.12%
Higher heating value	MJ/kg	-	46.200	40.047	38.431	39.889	-	39.952	40.82	−0.237%
Oxidation stability at 110 °C	°h	3 (min)	-	3.3	-	9.03	3.2	6.8	18.14	106%
Flash Point	°C	100–170	68.5	98	133	154	173	172	163.5	75.51%
Pour Point	°C	−15–16	6	12	3	9	4	9	4	−25%
Cloud point	°C	−3–12	17	25	3	24	5	21	3	−19.04%
Copper strip corrosion	--	3 (max)	1a	1a	-	1a	1a	1a	1a	-
Concentration sulfur residue	(*w*/*w*)%	-	0.0760	0.0092	-	0.0093	3.2	0.0079	0.03	−14.13%
Canradsons Carbon residue	(*w*/*w*)%	-	0.00002	0.00015	-	0.00034	-	0.00034	-	844.44%

[a,b,c] Result; WCME = waste cooking methyl ester; UCME = used cooking oil methyl ester; KOME = *Schleichera oleosa* methyl ester; KSME = Kusum oil methyl ester; WSME = waste cooking and *Schleichera oleosa* methyl ester and mixed (70:30); W70CI30 = waste cooking oil and *Calophyllum inopyllum* (70:30).

3.6. Analysis Low-Temperature Properties of Methyl Ester

Figure 3 shows the differential scanning calorimetry (DSC) analysis results on the low-temperature properties of the WCME and WSME biodiesel.

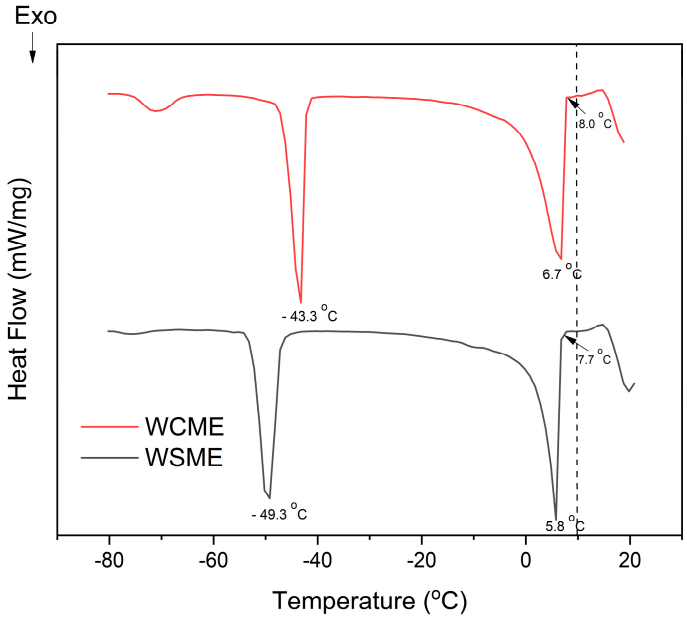

Figure 3. DSC curve of WCME and WSME.

Table 5 shows the results of data analysis for the DSC curves of WCME and WSME. The temperature at which wax crystals start to form is called T_{onset}. The slope of the peaks in DSC curves for WCME and WSME indicates the amount of wax deposition. ΔH refers to the energy change from the liquid to the solid phase of a substance [70]. The specific heat capacity (Cp) of a substance refers to the amount of heat energy required to raise the temperature of 1 kg by 1 °C for both WCME and WSME. Table 4 and Figure 3 show that WCME and WSME were 8.0 °C and 7.7 °C, respectively. These also show that adding SO oil to WCO oil affects the temperature at which wax crystals start to form, slightly restricting the formation of wax crystals. The DSC curves indicated that the T peaks of WCME and

WSME were 6.7 °C and 5.8 °C, respectively, with no significant differences in temperature peak and onset. Furthermore, the absolute ΔH of WCME (-7.1 J g^{-1}) was slightly lower than that of WSME, at -7.3 J g^{-1}.

Table 5. Analysis of the DSC graph WCME and WSME.

Sample	T_{onset} (°C)	T_{peak-1} (°C)	T_{peak-2} (°C)	ΔH (J g^{-1})	Cp (J/g °C)	Peak Area J/g
WCME	8.0	6.7	−43.3	−7.1	−0.03	−47.97
WSME	7.7	5.8	−49.3	−7.3	2.83	−63.73

3.7. GaschromatographyMass Spectrometry (GC-MS) Analysis of Biodiesel

There are two types of fatty acids, namely, saturated and unsaturated [71]. Unsaturated fatty acids are classified into two types, monounsaturated and polyunsaturated. Saturated fatty acids include stearic (18:1), palmitic (C16:0), and myristic acids (14:0) [45]. Furthermore, unsaturated fatty acids include oleic acid (C18:1), palmitoleic acid (C16:1), and gadoleic acid (C20:1) for containing a single, double bond along the carbon chain. Monounsaturated fatty acids, such as oleic acid (C18:1), palmitoleic acid (C16:1), and gadoleic acid (C20:1), have a double bond along the carbon chain. Polyunsaturated fatty acids, namely, linoleic acid (C18:2) and linolenic acid (C18:3), have at least two double bonds along the carbon chain [72]. Table 5 shows the methyl ester content derived from the esterification or transesterification process using a base catalyst KOH for WCO, SO, and WCOK30.

The results of the GC-MS test of WCME, KOME, and WSME are shown in Table 6. The palmitic acid content of WSME (51.08%) was higher than that of WCME and KOME (49.54% and 37.18%), respectively. On the other hand, the oleic acid content of WSME (36.25%) was slightly lower than that of WCME and KOME (38.16% and 45.56%), respectively. Biodiesel with high palmitic and oleic acid contents generally exhibits increased oxidation stability [58].

Table 6. Composition of FAME WCME, KOME, and WSME.

FAME (*w*/*w*) %	Carbon Chain	WCME [a]	WCME [73]	KOME [b]	Kusum [63]	WSME [c]	W70CI30 [7]
Caprylic	C8:0	-	25	-	-	-	-
Lauric	C12:0	-	3.2	-	-	-	-
Myristic	C14:0	-	1.73	0.46	0.01	0.60	0.64
Palmitic	C16:0	49.54	21.13	37.18	5–8	51.08	28.97
Arachidic	C20:0	-	-	-	-	-	-
Heneicosanoic	C21:0	-	1.79	-	-	-	-
Stearic	C18:0	5.55	3.43	-	2–6	4.90	7.40
Palmitoleic	C16:1	-	0.91		-	-	-
Heptadecanoic acid	C17:1	-	8.01	-	-	-	-
Eicosanoic	C20:1	-	2	-			
Oleic	C18:1	38.16	21.01	45.56	2–3	36.25	44.15
Linoleic	C18:2		11.77	7.54	5.56	-	14.11
Linolenic	C18:3	6.75	-	-	43–50	7.18	0.58

[a,b,c] Result; WCME = waste cooking methyl ester; UCME = used cooking oil methyl ester; KOME = *Schleichera oleosa* methyl ester; KSME = Kusum oil methyl ester; WSME = waste cooking and *Schleichera oleosa* methyl ester and mixed (70:30); W70CI30 = waste cooking oil and *Calophyllum inopyllum* (70:30).

WCME methyl ester lacks linolenic acid, whereas WSME and KOME have similar linolenic acid content. Moreover, WCME has a linoleic acid content of 6.75%, which is absent in WSME and KOME. Kumar et al. [58], propose that the high content of linolenic and linoleic acids in biodiesel encourages the susceptibility of oxidation. It was reported

that the WCME and KOME have a significant amount of linolenic acid, namely 7.18% and 7.54%, respectively. These amounts cause reduced oxidation stability. Lau et al. [8]. suggested that the oleic acid (18:1) and linoleic (18:2) are more stable than linolenic acid (C18:3) due to the presence of triple double bonds in its long 18-carbon chain.

The fatty acid composition of WCME, KOME, and WCME exhibits distinct differences in the proportion of saturated and unsaturated fatty acids. The total saturated fatty acid content of WCME (55.09%) was higher than that reported by Katre et al. [73], at 26.29%. The unsaturated fatty acid content of WCME was slightly higher (44.91%) as compared to those reported by Katre et al. [73], at 32.78%. In KOME, the saturated fatty acid content was 37.64%, which was higher than one reported by Sarkar et al. [63], approximately 14%, while the unsaturated fatty acid content was 53.1% and was higher than the value obtained by Sarkar et al. [63] at 51.56%. The mixed feedstock of WCO-*Schleichera oleosa* in a 70:30 ratio (WCOK30) showed a saturated fatty acid content of 51.58% and a total unsaturated fatty acid content of 66.28%. Despite this, the content of mono and polyunsaturated fatty acids was lower than that of saturated fatty acids. The content of polyunsaturated (43.43%) was higher than the monounsaturated type (7.18%).

3.8. Oxidation Stability (OS) of Biodiesel

Table 4 compares the physicochemical properties of this study's WCME, KOME, and WSME biodiesel. In the experiment, the oxidation stability of WCME, KOME, and WSME was measured and shown in Table 4. The oxidation stability of WCME was obtained at 3.3 h, which was consistent with the findings of Yesilyurt et al. [71]. On the other hand, KOME (9.03 h) showed higher oxidation stability than WCME (3.3 h), which was attributed to the high linolenic acid content of approximately 7.4% in KOME. The oxidation stability of WSME increased by 104% from 3.3 h to 6.8 h under the optimum conditions. These results correspond to Devi et al. [61], who reported that the addition of Thuja extract and TBHQ with a low concentration (100–250) ppm improved oxidation stability of the WCO biodiesel from 4.6 h to 6.79 h.

This improvement was attributed to the high content of palmitic acid in WSME as compared to WCME [58], as well as the presence of stearic and myristic fatty acids in WSME, which contributed to a better oxidation stability than WCME [67]. However, the high composition of saturated fatty acids in WSME can have a negative impact on the pour and cloud points but increases the oxidation stability [72]. It is worth noting that the samples' unsaturated ester composition was lower than methyl oleate and linoleic acids [45]. Furthermore, Uguz et al. [60] stated that differential scanning calorimetry (DSC) is an effective, rapid, and cost-efficient method for determining the oxidation stability of biodiesel. The process involves using DSC to characterise the initial temperature of the biodiesel sample crystallisation [74]. The cold flow properties of the fuel are then measured and compared to a temperature reference in an inert environment (nitrogen) as a function of temperature. DSC allows for observing various chemical processes related to changes in temperature, including oxidation, dissociation, dehydration, and decomposition, in biodiesel [60,74].

3.9. Effect of Catalyst Concentration

Figure 4 shows the influence of the concentration of KOH catalyst on the density and kinematic viscosity of WSME.

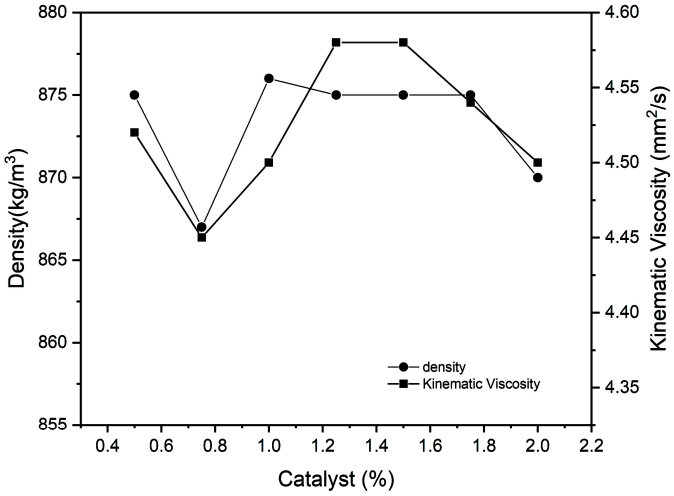

Figure 4. Effect catalyst concentrations for kinematic viscosity and density WSME.

The concentration of the catalyst varied from 0.5 wt.% to 2 wt.%, while all the other factors were kept constant. This change in catalyst concentration was observed to impact the kinematic viscosity and density of WCME. Interestingly, it was observed that increasing the catalyst concentration did not lead to any significant effect on the kinematic viscosity and density. At the optimal KOH catalyst concentration of 0.75%, the kinematic viscosity and density were measured to be 4.35 mm^2/s and 0.857 kg/m^3, respectively.

It is worth noting that elevated catalyst concentrations (1.75 wt.% and 2 wt.%) led to a decreased kinematic viscosity and density. However, an excessive amount of catalysts not only causes the low conversion of methyl esters but also results in emulsions and increased viscosity [75]. The kinematic viscosity of WSME was lower than that of WCME and KOME. The kinematic viscosity values for WCME, KOME, and WSME complied with the ASTM 6751 standards. It was observed that prolonged frying time, high temperature, and salt content can progressively decrease the density, calorific value, viscosity, cloud, and pour points of WCO biodiesel [67].

3.10. Effect of Reaction Times and Catalyst Concentration on Methyl Ester Yield

The study examined the impact of varying reaction times of 30 min between 60 min to 120 min and increasing the concentration of KOH catalyst on WCOK30 methyl ester from 0.5% vol to 2% vol. Meanwhile, other factors were kept constant, including a methanol/oil ratio of 10:1, a reaction temperature of 60 °C, and an agitation speed of 1000 rpm, as shown in Figure 5.

The high catalytic activity of KOH makes it the preferred choice as a homogeneous catalyst in producing methyl esters. The optimal yield of methyl ester (92.4%) was obtained using a catalyst concentration of 0.5 wt.% and a reaction time of 90 min. However, a catalyst concentration of 0.75 wt.% and a reaction time of 120 min also resulted in a high methyl ester yield (90%). According to Silitonga et al. [76], a reaction time of less than 90 min was found to be optimal for achieving high yield, while a reaction time of 60 min produced a yield of 83%.

When the processing time is prolonged, a reversible transesterification reaction may occur, leading to soap formation and reduced biodiesel production. High temperatures during extended reaction times tend to hydrolyse the biodiesel [65]. Generally, a processing time of up to 2 h does not significantly increase biodiesel yield. Based on Figure 4, the optimum processing time for producing biodiesel is 60 min for almost all the various amounts of catalyst.

In general, raising the catalyst concentrations (1 wt.% and 2 wt.%) and prolonging the reaction time does not significantly affect the yield of methyl ester. On the other hand, utilising a higher KOH catalyst concentration during the transesterification process results

in excess soap formation, thereby reducing methyl ester yield [75]. Adding a catalyst of more than 1% by weight does not enhance biodiesel conversion and may increase production costs. An excessive amount of KOH catalyst concentration causes the formation of emulsions and gel [77].

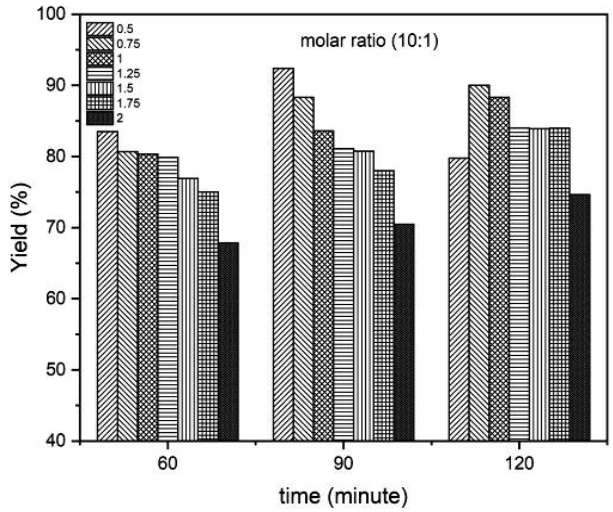

Figure 5. Effect of reaction time and catalyst concentration on WSME yield with molar ratio to oil (10:1).

3.11. Effect of Methanol to Oil Molar Ratio on Methyl Ester Yield

The methyl ester yield for WCOK30 was compared based on parameters, such as methanol to oil molar ratio and reaction time, as shown in Figures 6 and 7. The methanol to oil molar ratio was examined at three levels (8:1, 10:1, and 12:1), while the concentration of the KOH catalyst varied from 0.5 wt.% to 2 wt.%. Other factors were kept constant, as shown in Figure 6.

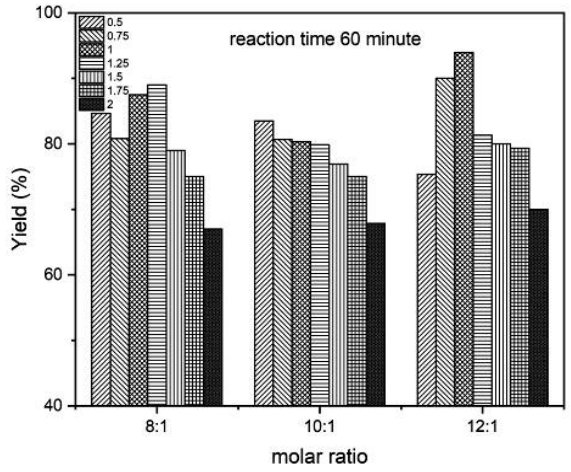

Figure 6. Effect of catalyst concentration and methanol to oil ratio on WSME yield at reaction time 60 min.

The study utilised a reaction temperature, time, and stirring or agitation speeds of 60 °C, 60 min, and 1000 rpm, respectively. The reaction temperature was maintained at 60 °C, below the methanol's boiling point (64.7 °C). Raising the temperature of transesterification to 70 °C may lead to a reduced oil conversion and increased saponification reaction [77]. The effect of the methanol to oil molar ratio on the yield of WSME is shown in Figure 7. The optimum condition was found to be a KOH catalyst of 1 vol% and a methanol to oil molar ratio of 10:1, resulting in the highest yield of 94%. The highest yield for the

lowest methanol to oil molar ratio (8:1) was 89%, more than the yield of 83% obtained for the ratio of 10:1. The varying amount of KOH catalyst and methanol to oil molar ratio (8:1, 10:1, and 12:1) at a reaction time of 90 min was compared to the optimum yield of methyl ester of WSME as shown in Figure 7.

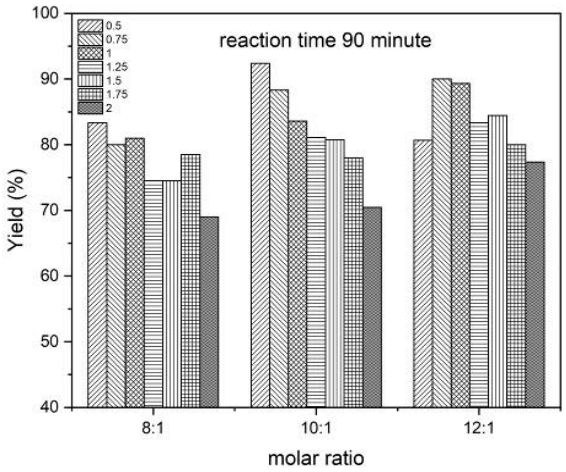

Figure 7. Effect of catalyst concentration and methanol to oil ratio on WSME yield at reaction time 90 min.

Based on the data presented in Figure 7, it can be inferred that the most effective methanol to oil molar ratio for producing WCOK30 was 10:1. This ratio resulted in the highest yield of 92.4% when using a 0.5 wt.% concentration of catalyst and reaction time of 90 min. The results suggested that the molar ratios 12:1 and 8:1 followed behind in effectiveness. Mohadesi et al. [78] also found similar results, with an optimal methanol to oil ratio of 9.4:1. However, excess methanol can lead to some issues, such as increase in the solubility of glycerol in esters, which can result in foam formation. The excess methanol increases precipitation time, as some glycerides may not react during transesterification [77]. Asl et al. [29] stated that excess methanol can decrease the product yield, as it causes biodiesel to become a water phase during washing. Surplus methanol can also lead to a significant solubility of glycerol in alcohol, making it more difficult to separate.

3.12. FTIR Fourier-Transform Infrared (FT-IR) Spectroscopy Analysis

Analysing the adsorption layer created by its process can be effectively carried out by using FTIR (Fourier Transform Infrared) spectroscopy. In this context, FT-IR spectra were utilised to compare WCOK30 crude oil with WSME biodiesel. Figure 8 shows the FTIR spectra for crude oil WCOK30 and WSME biodiesel, enabling a comparison between the two.

In Table 7, details related to the wave number, absorption intensity, vibration type, and group attribute of WCO crude oil and WSME are presented for reference. The comparison of WCOK30 crude oil and WSME by using the FTIR spectrum is shown in Figure 8, with the blue and red lines representing the spectra of crude oil and biodiesel, respectively. The absorption peaks observed in the spectra indicated the presence of a methyl group at 2921.60 cm^{-1} and 2852.59 cm^{-1}. Milano et al. [23] found results similar to those in this study (2923 cm^{-1}), which described strong CH stretching. Figure 8 shows the stretching peak observed at 1741 cm^{-1} in the crude oil spectrum, corresponding to the functional ester group (C=O) present in WSME [49]. The results found in this study related to the stretching of the CO double bonds are similar to the results reported by Milano et al. (1742 cm^{-1}) [23].

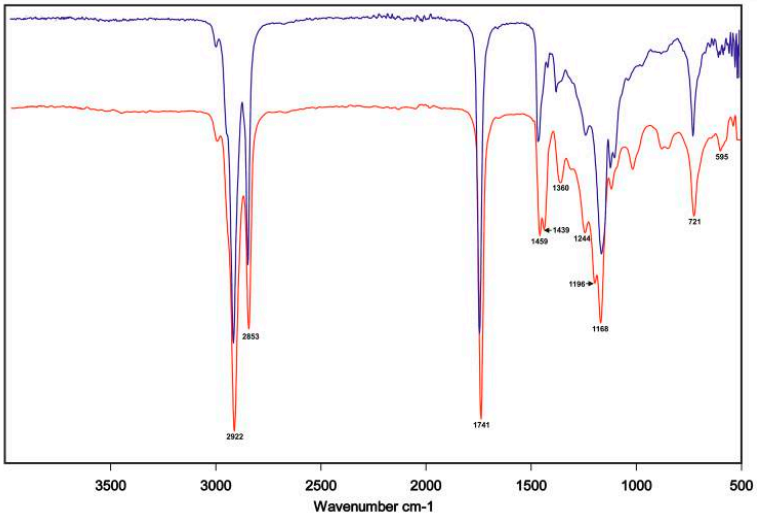

Figure 8. FTIR spectra of the crude oil WCOK30 and WCME.

Table 7. Spectra FTIR of crude oil WCOK30 and WSME.

Wavenumber (cm^{-1})	Group Attribution	Vibration Type	Absorption Intensity
2922	=C-H	Asymmetric stretching vibration	Strong
2853	$-CH_2$	Symmetric stretching vibration	Strong
1741	-C=O	Stretching	Strong
1459	$-CH_2$	Shear type vibration	Weak
1439	$-CH_3$	Shear type vibration	Middling
1244	$-CH_3$	Bending vibration	Weak
1196	C-O-C	Anti-symmetric stretching vibration	Middling
1168	C-O-C	Anti-symmetric stretching vibration	Middling
721	$-CH_2$	Plane rocking vibration	Weak

Distinctive peaks at different wave numbers can be observed in the FTIR spectra of refined oil and biodiesel. The peak at 1439 cm^{-1} and 1196 cm^{-1} in the biodiesel spectrum corresponds to the asymmetric stretching of CH_3, which is not present in the refined oil spectrum [23,79]. This is a typical methyl ester peak, as reported by previous studies by Asla et al. [29]. Milano et al. [23] reported a similar new absorption peak at 1436 cm^{-1} and 1195 cm^{-1}. On the other hand, the peak observed at 1377 cm^{-1} in the refined oil spectrum corresponded to the glycerol group O-CH_2 (mono-, di-, and triglycerides), which is absent in the FAME (Fatty Acid Methyl Ester) spectrum [79]. Similar results were also found by Tan et al. [80], wherein the peak was observed at 1377 cm^{-1} Additionally, the absorbance at 1196 cm^{-1} indicated the stretching of –C-O, a characteristic feature of biodiesel [79]. In line with the findings of Bai et al. [81], the stretching vibration peak in the 1196 cm^{-1} band is a characteristic feature of biodiesel.

Figure 8 shows the presence of ester (C-O) at a wavelength ranging between 1300 cm^{-1} and 1000 cm^{-1}, as observed in the FTIR spectra. The similarity in the chemical properties of methyl esters and triglycerides is reflected in the similar FTIR spectra of crude oil and WSME biodiesel, as shown in Figure 8.

The differences between WCOK30 and WSME can be observed in their FTIR spectra. There was a shift in the peak position at 1743.69 cm^{-1}, 1376.98 cm^{-1}, 1159.66 cm^{-1}, 1116.52 cm^{-1}, 721.56 cm^{-1} to 1741.63 cm^{-1}, 1368.52 cm^{-1}, 1168.52 cm^{-1}, 1017.11 cm^{-1}, 721.87 cm^{-1} in each sample. The emergence of new peaks at 1439.54 cm^{-1} and

1196.25 cm^{-1} as well as the disappearance of peaks at 1463.79 cm^{-1} and 1116.52 cm^{-1} in the WCOK30 spectrum indicated the formation of fatty acid methyl esters O-CH_3. The peak at 1439 cm^{-1} in the spectrum indicated the asymmetric deformation of O-CH_3 methoxide, which confirmed the formation of methyl esters [81].

4. Conclusions

This study aimed to improve the flash, cloud points, and oxidation stability of biodiesel by mixing *Schleichera oleosa* oil with WCO in a ratio of 70:30. Its focus was to determine the optimal methanol-to-oil molar ratio and reaction time for the highest methyl ester yield of the mixed cooking oils and to investigate the effect of catalyst concentration on the physicochemical properties. The results showed that the highest methyl ester yield of 94% was achieved with a catalyst concentration of 1 wt.%, a molar ratio of 12:1, and a reaction time of 60 min. By utilising a catalyst concentration of 0.75 wt.% and a total esterification and transesterification time of 120 min, the density and kinematic viscosity of the biodiesel were found to be 0.857 kg/m^3, and 4.35 mm^2/s, respectively. The initial temperature of biodiesel crystallisation as measured by DSC was found to be similar to the pour point. After the transesterification process, the oxidation stability of WSME increased by 103%, while the flash point and the pour point increased by 75.51% and 25%, respectively. In conclusion, the physiochemical properties of WSME (density, viscosity, pour point, flash point) met the ASTM D6751 standards. Future study should investigate the optimal balance of saturated and unsaturated fats to improve biodiesel's oxidation stability and cold flow properties with respect to varying mixtures of different crude oils.

Author Contributions: Conceptualisation, S.S. and A.S.S.; methodology, A.S.S.; software, M.S.; validation, A.S.S., M.S. and I.A.; formal analysis, M.S.; investigation, S.S.; resources, S.S.; data curation, S.S.; writing—original draft preparation, S.S.; writing—review and editing, A.S.S.; visualisation, M.S.; supervision, I.A.; project administration, S.S.; funding acquisition, I.A. All authors have read and agreed to the published version of the manuscript.

Funding: The authors are grateful to the Ministry of Education, Culture, Research, and Technology, for financing this study through the Doctoral Dissertation Grant Scheme of the University Sumatera Utara with Contract number 013/UN5.2.3.1/PPM/KP-DRTPM/TI/2022. The authors also wish to thank University of Technology Sydney, Sydney, Australia (Strategy Research Support Funding 2023) and Politeknik Negeri Medan, Medan Indonesia (DIPA POLMED 2023).

Data Availability Statement: Data is contained within article.

Acknowledgments: The authors are also grateful to the Politeknik Negeri Medan for using renewable energy laboratory facilities to produce biodiesel and to Bella Nurulita for her assistance.

Conflicts of Interest: The authors declare no conflict of interest.

Abbreviations

ASTM	American Society for Testing and Materials
CP	Cloud Point
DSC	Differential Scanning Calorimetry
EN	European standard
FAME	Fatty acid Methyl Ester
FP	Flash Point
KOME	*Schleichera oleosa* methyl ester
OS	Oxidation Stability
PP	Pour Point
SO	Crude oil *Schleichera oleosa* oil
WCME	Waste cooking methyl ester
WCO	Crude Waste Cooking Oil
WCOK30	Crude Waste Cooking Oil and *Schleichera oleosa* oil mixed
WSME	Waste Cooking Oil and *Schleichera oleosa* oil and mixed methyl ester

References

1. Vidigal, I.G.; Siqueira, A.F.; Melo, M.P.; Giordani, D.S.; da Silva, M.L.; Cavalcanti, E.H.; Ferreira, A.L. Applications of an electronic nose in the prediction of oxidative stability of stored biodiesel derived from soybean and waste cooking oil. *Fuel* **2021**, *284*, 119024. [CrossRef] [PubMed]
2. Mortaza, A.; Soleiman, S.; Tabatabaei, M.; Soufiyan, M.M. Multi-objective exergetic and technical optimisation of a piezoelectric ultrasonic reactor applied to synthesise biodiesel from waste cooking oil (WCO) using soft computing techniques. *Fuel* **2019**, *235*, 100–112.
3. Aitbelale, R.; Abala, I.; Alaoui, F.E.M.; Sahibed-Dine, A.; Rujas, N.M.; Aguilar, F. Characterization and determination of thermodynamic properties of waste cooking oil biodiesel: Experimental, correlation and modeling density over a wide temperature range up to 393.15 and pressure up to 140 MPa. *Fluid Phase Equilibria* **2019**, *497*, 87–96. [CrossRef]
4. Hu, Z.; Fu, J.; Gao, X.; Lin, P.; Zhang, Y.; Tan, P.; Lou, D. Waste cooking oil biodiesel and petroleum diesel soot from diesel bus: A comparison of morphology, nanostructure, functional group composition and oxidation reactivity. *Fuel* **2022**, *321*, 124019. [CrossRef]
5. Sebayang, A.H.; Milano, J.; Alfansuri, M.; Silitonga, A.S.; Kusumo, F.; Prahmana, R.A.; Fayaz, H.; Zamri, M.F.M.A. Modelling and prediction approach for engine performance and exhaust emission based on artificial intelligence of sterculia foetida biodiesel. *Energy Rep.* **2022**, *8*, 8333–8345. [CrossRef]
6. Helmi, M.; Tahvildari, K.; Hemmati, A.; Safekordi, A. Phosphomolybdic acid/graphene oxide as novel green catalyst using for biodiesel production from waste cooking oil via electrolysis method: Optimisation using with response surface methodology (RSM). *Fuel* **2021**, *287*, 119528. [CrossRef]
7. Milano, J.; Ong, H.C.; Masjuki, H.H.; Silitonga, A.S.; Chen, W.-H.; Kusumo, F.; Dharma, S.; Sebayang, A.H. Optimisation of biodiesel production by microwave irradiation-assisted transesterification for waste cooking oil-*Calophyllum inophyllum* oil via response surface methodology. *Energy Convers. Manag.* **2018**, *158*, 400–415. [CrossRef]
8. Lau, C.H.; Gan, S.; Lau, H.L.N.; Lee, L.Y.; Thangalazhy-Gopakumar, S.; Ng, H.K. Insights into the effectiveness of synthetic and natural additives in improving biodiesel oxidation stability. *Sustain. Energy Technol. Assess.* **2022**, *52*, 102296. [CrossRef]
9. Dharma, S.; Ong, H.C.; Masjuki, H.; Sebayang, A.; Silitonga, A. An overview of engine durability and compatibility using biodiesel–bioethanol–diesel blends in compression-ignition engines. *Energy Convers. Manag.* **2016**, *128*, 66–81. [CrossRef]
10. Cordero-Ravelo, V.; Schallenberg-Rodriguez, J. Biodiesel production as a solution to waste cooking oil (WCO) disposal. Will any type of WCO do for a transesterification process? A quality assessment. *J. Environ. Manag.* **2018**, *228*, 117–129. [CrossRef]
11. Guo, J.; Sun, S.; Liu, J. Conversion of waste frying palm oil into biodiesel using free lipase A from Candida antarctica as a novel catalyst. *Fuel* **2020**, *267*, 117323. [CrossRef]
12. Mujtaba, M.; Masjuki, H.; Kalam, M.; Noor, F.; Farooq, M.; Ong, H.C.; Gul, M.; Soudagar, M.E.M.; Bashir, S.; Rizwanul Fattah, I. Effect of additivized biodiesel blends on diesel engine performance, emission, tribological characteristics, and lubricant tribology. *Energies* **2020**, *13*, 3375. [CrossRef]
13. Ayetor, G.K.; Sunnu, A.; Parbey, J. Effect of biodiesel production parameters on viscosity and yield of methyl esters: Jatropha curcas, Elaeis guineensis and Cocos nucifera. *Alex. Eng. J.* **2015**, *54*, 1285–1290. [CrossRef]
14. Chinnamma, M.; Bhasker, S.; Madhav, H.; Devasia, R.M.; Shashidharan, A.; Pillai, B.C.; Thevannoor, P. Production of coconut methyl ester (CME) and glycerol from coconut (Cocos nucifera) oil and the functional feasibility of CME as biofuel in diesel engine. *Fuel* **2015**, *140*, 4–9. [CrossRef]
15. Niyas, M.M.; Shaija, A. Performance evaluation of diesel engine using biodiesels from waste coconut, sunflower, and palm cooking oils, and their hybrids. *Sustain. Energy Technol. Assess.* **2022**, *53*, 102681.
16. Colombo, K.; Santos, M.; Ender, L.; Barros, A.C. Production of biodiesel from soybean oil and methanol, catalysed by calcium oxide in a recycle reactor. *S. Afr. J. Chem. Eng.* **2019**, *28*, 19–25. [CrossRef]
17. Elkelawy, M.; Bastawissi, H.A.-E.; Esmaeil, K.K.; Radwan, A.M.; Panchal, H.; Sadasivuni, K.K.; Suresh, M.; Israr, M. Maximization of biodiesel production from sunflower and soybean oils and prediction of diesel engine performance and emission characteristics through response surface methodology. *Fuel* **2020**, *266*, 117072. [CrossRef]
18. Silitonga, A.S.; Masjuki, H.H.; Ong, H.C.; Kusumo, F.; Mahlia, T.M.I.; Bahar, A.H. Pilot-scale production and the physicochemical properties of palm and Calophyllum inophyllum biodiesels and their blends. *J. Clean. Prod.* **2016**, *126*, 654–666. [CrossRef]
19. Silitonga, A.S.; Ong, H.C.; Mahlia, T.M.I.; Masjuki, H.H.; Chong, W.T. Biodiesel conversion from high FFA crude jatropha curcas, calophyllum inophyllum and ceiba pentandra oil. *Energy Procedia* **2014**, *61*, 480–483. [CrossRef]
20. Silitonga, A.S.; Mahlia, T.M.I.; Ong, H.C.; Riayatsyah, T.M.I.; Kusumo, F.; Husin, I.; Dharma, S.; Gumilang, D. A comparative study of biodiesel production methods for Reutealis trisperma biodiesel. *Energy Sources Part A Recovery Util. Environ. Eff.* **2017**, *39*, 2006–2014. [CrossRef]
21. Jamaluddin, N.A.M.; Riayatsyah, T.M.I.; Silitonga, A.S.; Mofijur, M.; Shamsuddin, A.H.; Ong, H.C.; Mahlia, T.M.I.; Rahman, S.M.A. Techno-economic analysis and physicochemical properties of Ceiba pentandra as second-generation biodiesel based on ASTM D6751 and EN 14214. *Processes* **2019**, *7*, 636. [CrossRef]
22. Uyumaz, A. Combustion, performance and emission characteristics of a DI diesel engine fueled with mustard oil biodiesel fuel blends at different engine loads. *Fuel* **2018**, *212*, 256–267. [CrossRef]

23. Milano, J.; Ong, H.C.; Masjuki, H.H.; Silitonga, A.S.; Kusumo, F.; Dharma, S.; Sebayang, A.H.; Cheah, M.Y.; Wang, C.-T. Physicochemical property enhancement of biodiesel synthesis from hybrid feedstocks of waste cooking vegetable oil and Beauty leaf oil through optimised alkaline-catalysed transesterification. *Waste Manag.* **2018**, *80*, 435–449. [CrossRef]
24. Sudalaiyandi, K.; Alagar, K.; VJ, M.P.; Madhu, P. Performance and emission characteristics of diesel engine fueled with ternary blends of linseed and rubber seed oil biodiesel. *Fuel* **2021**, *285*, 119255.
25. Alptekin, E.; Canakci, M.; Sanli, H. Biodiesel production from vegetable oil and waste animal fats in a pilot plant. *Waste Manag.* **2014**, *34*, 2146–2154. [CrossRef]
26. Milano, J.; Shamsuddin, A.H.; Silitonga, A.; Sebayang, A.; Siregar, M.A.; Masjuki, H.; Pulungan, M.A.; Chia, S.R.; Zamri, M. Tribological study on the biodiesel produced from waste cooking oil, waste cooking oil blend with Calophyllum inophyllum and its diesel blends on lubricant oil. *Energy Rep.* **2022**, *8*, 1578–1590. [CrossRef]
27. Ideris, F.; Zamri, M.F.M.A.; Shamsuddin, A.H.; Nomanbhay, S.; Kusumo, F.; Fattah, I.M.R.; Mahlia, T.M.I. Progress on Conventional and Advanced Techniques of In Situ Transesterification of Microalgae Lipids for Biodiesel Production. *Energies* **2022**, *15*, 7190. [CrossRef]
28. Ong, H.C.; Tiong, Y.W.; Goh, B.H.H.; Gan, Y.Y.; Mofijur, M.; Fattah, I.M.R.; Chong, C.T.; Alam, M.A.; Lee, H.V.; Silitonga, A.S. Recent advances in biodiesel production from agricultural products and microalgae using ionic liquids: Opportunities and challenges. *Energy Convers. Manag.* **2021**, *228*, 113647. [CrossRef]
29. Asl, M.A.; Tahvildari, K.; Bigdeli, T. Eco-friendly synthesis of biodiesel from WCO by using electrolysis technique with graphite electrodes. *Fuel* **2020**, *270*, 117582. [CrossRef]
30. Isah, A.G.; Faruk, A.A.; Musa, U.G.; Mohammed, U.; Alhassan, M.; Abdullahi, U.B.; Damian, A.T. Oxidation stability and cold flow properties of biodiesel synthesised from castor oil: Influence of alkaline catalysts type and purification techniques. *Mater. Today Proc.* **2022**, *57*, 748–752. [CrossRef]
31. Fonseca, J.M.; Teleken, J.G.; de Cinque Almeida, V.; da Silva, C. Biodiesel from waste frying oils: Methods of production and purification. *Energy Convers. Manag.* **2019**, *184*, 205–218. [CrossRef]
32. Kuniyil, M.; Kumar, J.V.K.; Adil, S.F.; Assal, M.E.S.; Khan, M.R.; Warthan, M.A.; Siddiqui, A.; Rafiq, M.H. Production of biodiesel from waste cooking oil using ZnCuO/N-doped graphene nanocomposite as an efficient heterogeneous catalyst. *Arab. J. Chem.* **2021**, *14*, 102982. [CrossRef]
33. Anilkumar, R.; Gupta, S.V.Y.; Virendra, K. Rathod. Enhancement in biodiesel production using waste cooking oil and calcium diglyceroxide as a heterogeneous catalyst in presence of ultrasound. *Fuel* **2015**, *158*, 800–806. [CrossRef]
34. Kurniati, S.; Soeparman, S.; Yuwono, S.S.; Hakim, L.; Syam, S. A Novel Process for Production of Calophyllum Inophyllum Biodiesel with Electromagnetic Induction. *Energies* **2019**, *12*, 383. [CrossRef]
35. Binhayeeding, N.; Klomklao, S.; Prasertsan, P.; Sangkharak, K. Improvement of biodiesel production using waste cooking oil and applying single and mixed immobilised lipases on polyhydroxyalkanoate. *Renew. Energy* **2020**, *162*, 1819–1827. [CrossRef]
36. Zhang, H.; Tian, F.; Xu, L.; Peng, R.; Li, Y.; Deng, J. Batch and continuous esterification for the direct synthesis of high qualified biodiesel from waste cooking oils (WCO) with Amberlyst-15/Poly (vinylalcohol) membrane as a bifunctional catalyst. *Chem. Eng. J.* **2020**, *388*, 124214. [CrossRef]
37. Pradhan, P.C.S.; Chakraborty, R. Optimization of infrared radiated fast and energy-efficient biodiesel production from waste mustard oil catalysed by Amberlyst 15: Engine performance and emission quality assessments. *Fuel* **2016**, *173*, 60–68. [CrossRef]
38. Singh, D.S.D.; Soni, S.L.; Inda, C.S.; Sharma, S.; Sharma, P.K.; Jhalani, A. A comprehensive review of biodiesel production from waste cooking oil and its use as fuel in compression ignition engines: 3rd generation cleaner feedstock. *J. Clean. Prod.* **2021**, *307*, 127299. [CrossRef]
39. Naveen, S.; Gopinath, K.P.; Malolan, R.; Ramesh, S.J.; Aakriti, K.; Arun, J. Novel Solar Parabolic Trough Collector cum Reactor for the Production of Biodiesel from Waste Cooking Oil using Calcium Oxide catalyst derived from seashells waste. *Chem. Eng. Process. Process Intensif.* **2020**, *157*, 108145. [CrossRef]
40. Pölczmann, G.; Tóth, O.; Beck, Á.; Hancsók, J. Investigation of storage stability of diesel fuels containing biodiesel produced from waste cooking oil. *J. Clean. Prod.* **2016**, *111*, 85–92. [CrossRef]
41. Wang, J.C.L.; Han, S. Effect of polymeric cold flow improvers on flow properties of biodiesel from waste cooking oil. *Fuel* **2014**, *117*, 876–881. [CrossRef]
42. Bharti, R.B.S. Green tea (Camellia assamica) extract as an antioxidant additive to enhance the oxidation stability of biodiesel synthesised from waste cooking oil. *Fuel* **2020**, *262*, 116658. [CrossRef]
43. Nanihar, N.K.A.; Hakim, F.; Sunar, N.M.; Manshoor, B.; Zaman, I. Influences of Storage Duration on the Fuel Properties of Biodiesel derived from Jatropha and Waste Cooking Oil. *IOP Conf. Ser. J. Phys. Conf. Ser.* **2018**, *1049*, 012091. [CrossRef]
44. Khounani, Z.; Hosseinzadeh-Bandbafha, H.; Nizami, A.-S.; Sulaiman, A.; Goli, S.A.H.; Tavassoli-Kafrani, E.; Ghaffari, A.; Rajaeifar, M.A.; Kim, K.-H.; Talebi, A.F.; et al. Unlocking the potential of walnut husk extract in the production of waste cooking oil-based biodiesel. *Renew. Sustain. Energy Rev.* **2020**, *119*, 109588. [CrossRef]
45. Fu, J.; Turn, S.Q.; Takushi, B.M.; Kawamata, C.L. Storage and oxidation stabilities of biodiesel derived from waste cooking oil. *Fuel* **2016**, *167*, 89–97. [CrossRef]
46. Amran, N.A.; Bello, U.; Ruslan, M.S.H. The role of antioxidants in improving biodiesel's oxidative stability, poor cold flow properties, and the effects of the duo on engine performance: A review. *Heliyon* **2022**, *8*, e09846. [CrossRef]

47. Rajamohan, S.; Gopal, A.H.; Muralidharan, K.R.; Huang, Z.; Paramasivam, B.; Ayyasamy, T.; Nguyen, X.P.; Le, A.T.; Hoang, A.T. Evaluation of oxidation stability and engine behaviors operated by Prosopis juliflora biodiesel/diesel fuel blends with presence of synthetic antioxidant. *Sustain. Energy Technol. Assess.* **2022**, *52*, 102086. [CrossRef]
48. Chrysikou, S.B.L.P. Oxidative stability of waste cooking oil and white diesel upon storage at room temperature. *Bioresour. Technol.* **2012**, *126*, 341–344. [CrossRef]
49. Ideris, F.; Shamsuddin, A.H.; Nomanbhay, S.; Kusumo, F.; Silitonga, A.S.; Ong, M.Y.; Ong, H.C.; Mahlia, T.M.I. Optimisation of ultrasound-assisted oil extraction from Canarium odontophyllum kernel as a novel biodiesel feedstock. *J. Clean. Prod.* **2021**, *288*, 125563. [CrossRef]
50. Agarwal, A.K.; Khurana, D.; Dhar, A. Improving oxidation stability of biodiesels derived from Karanja, Neem and Jatropha: Step forward in the direction of commercialisation. *J. Clean. Prod.* **2015**, *107*, 646–652. [CrossRef]
51. Rashedul, H.; Masjuki, H.; Kalam, M.; Teoh, Y.; How, H.; Fattah, I.R. Effect of antioxidant on the oxidation stability and combustion–performance–emission characteristics of a diesel engine fueled with diesel–biodiesel blend. *Energy Convers. Manag.* **2015**, *106*, 849–858. [CrossRef]
52. Xue, Y.; Zhao, W.; Ma, P.; Zhao, Z.; Xu, G.; Yang, C.; Chen, H.; Lin, H.; Han, S. Ternary blends of biodiesel with petro-diesel and diesel from direct coal liquefaction for improving the cold flow properties of waste cooking oil biodiesel. *Fuel* **2016**, *177*, 46–52. [CrossRef]
53. Ong, H.C.; Milano, J.; Silitonga, A.S.; Hassan, M.H.; Shamsuddin, A.H.; Wang, C.-T.; Mahlia, T.M.I.; Siswantoro, J.; Kusumo, F.; Sutrisno, J. Biodiesel production from Calophyllum inophyllum-Ceiba pentandra oil mixture: Optimisation and characterisation. *J. Clean. Prod.* **2019**, *219*, 183–198. [CrossRef]
54. Dharma, S.; Hassan, M.H.; Ong, H.C.; Sebayang, A.H.; Silitonga, A.S.; Kusumo, F.; Milano, J. Experimental study and prediction of the performance and exhaust emissions of mixed Jatropha curcas-Ceiba pentandra biodiesel blends in diesel engine using artificial neural networks. *J. Clean. Prod.* **2017**, *164*, 618–633. [CrossRef]
55. Kassem, Y.H.Ç. Effects of storage under different conditions on the fuel properties of biodiesel admixtures derived from waste frying and canola oils. *Biomass Convers. Biorefinery* **2018**, *8*, 825–845. [CrossRef]
56. Zhang, X.; Li, N.; Wei, Z.; Dai, B.; Lin, H.; Han, S. Enhanced the Effects on Improving the Cold Flow Properties and Oxidative Stability of Diesel-Biodiesel Blends by Grafting Antioxidant on Pma Type Pour Point Depressant. *Fuel Process. Technol.* **2022**, *238*, 107483. [CrossRef]
57. Jain, S.S.; Sharma, M.P. Effect of metal contents on oxidation stability of biodiesel/diesel blends. *Fuel* **2014**, *116*, 14–18. [CrossRef]
58. Kumar, N. Oxidative stability of biodiesel: Causes, effects and prevention. *Fuel* **2017**, *190*, 328–350. [CrossRef]
59. Serqueira, D.S.; Pereira, J.F.; Squissato, A.L.; Rodrigues, M.A.; Lima, R.C.; Faria, A.M.; Richter, E.M.; Munoz, R.A. Oxidative stability and corrosivity of biodiesel produced from residual cooking oil exposed to copper and carbon steel under simulated storage conditions: Dual effect of antioxidants. *Renew. Energy* **2021**, *164*, 1485–1495. [CrossRef]
60. Uğuz, G.; Atabani, A.; Mohammed, M.; Shobana, S.; Uğuz, S.; Kumar, G.; Al-Muhtaseb, A.H. Fuel stability of biodiesel from waste cooking oil: A comparative evaluation with various antioxidants using FT-IR and DSC techniques. *Biocatal. Agric. Biotechnol.* **2019**, *21*, 101283. [CrossRef]
61. Devi, A.; Das, V.K.; Deka, D. A green approach for enhancing oxidation stability including long storage periods of biodiesel via Thuja oreantalis L. as an antioxidant additive. *Fuel* **2019**, *253*, 1264–1273. [CrossRef]
62. Sun, B.; Zhang, X.; Zhao, Y.; Chen, F.; Ren, F.; Lin, H.; Xue, Y.; Han, S. Bifunctional additive phenolic acids grafted ethylene-vinyl acetate copolymers for improving the cold flow properties and oxidative stability of waste cooking oil biodiesel-diesel blends. *Fuel* **2023**, *332*, 126005. [CrossRef]
63. Sarkar, P.K.; Sinha, A.; Das, B.; Dhakar, M.; Shinde, R.; Chakrabarti, A.; Yadav, V.; Bhatt, B. Kusum (Schleichera oleosa (Lour.) Oken): A potential multipurpose tree species, it's future perspective and the way forward. *Acta Ecol. Sin.* **2022**, *42*, 565–571. [CrossRef]
64. Sakthivel, R.; Ramesh, K.; Purnachandran, R.; Shameer, P.M. A review on the properties, performance and emission aspects of the third generation biodiesels. *Renew. Sustain. Energy Rev.* **2018**, *82*, 2970–2992. [CrossRef]
65. Rekhate, C.; Prajapati, A.K. Production, engine performance, combustion, emission characteristics and economic feasibility of biodiesel from waste cooking oil: A review. *Environ. Qual. Manag.* **2019**, *29*, 7–35. [CrossRef]
66. Doğan, T.H. The testing of the effects of cooking conditions on the quality of biodiesel produced from waste cooking oils. *Renew. Energy* **2016**, *94*, 466–473. [CrossRef]
67. Damanik, N.; Ong, H.C.; Chong, W.; Silitonga, A. Biodiesel production from Calophyllum inophyllum−palm mixed oil. *Energy Sources Part A Recovery Util. Environ. Eff.* **2017**, *39*, 1283–1289. [CrossRef]
68. Zhang, X.; Li, N.; Wei, Z.; Dai, B.; Han, S. Synthesis and evaluation of bifunctional polymeric agent for improving cold flow properties and oxidation stability of diesel-biodiesel blends. *Renew. Energy* **2022**, *196*, 737–748. [CrossRef]
69. Yesilyurt, M.K. The effects of the fuel injection pressure on the performance and emission characteristics of a diesel engine fuelled with waste cooking oil biodiesel-diesel blends. *Renew. Energy* **2019**, *132*, 649–666. [CrossRef]
70. Sia, C.B.; Kansedo, J.; Tan, Y.H.; Lee, K.T. Evaluation on biodiesel cold flow properties, oxidative stability and enhancement strategies: A review. *Biocatal. Agric. Biotechnol.* **2020**, *24*, 101514. [CrossRef]

71. Katre, G.; Raskar, S.; Zinjarde, S.; Kumar, V.R.; Kulkarni, B.; RaviKumar, A. Optimisation of the in situ transesterification step for biodiesel production using biomass of Yarrowia lipolytica NCIM 3589 grown on waste cooking oil. *Energy* **2018**, *142*, 944–952. [CrossRef]
72. Atabani, A.; Shobana, S.; Mohammed, M.; Uğuz, G.; Kumar, G.; Arvindnarayan, S.; Aslam, M.; Al-Muhtaseb, A.H. Integrated valorisation of waste cooking oil and spent coffee grounds for biodiesel production: Blending with higher alcohols. *Fuel* **2019**, *244*, 419–430. [CrossRef]
73. Silitonga, A.; Masjuki, H.; Ong, H.C.; Yusaf, T.; Kusumo, F.; Mahlia, T. Synthesis and optimisation of Hevea brasiliensis and Ricinus communis as feedstock for biodiesel production. *Ind. Crops Prod.* **2016**, *85*, 274–286. [CrossRef]
74. Rabie, A.M.; Shaban, M.; Abukhadra, M.R.; Hosny, R.; Ahmed, S.A.; Negm, N.A. Diatomite supported by CaO/MgO nanocomposite as heterogeneous catalyst for biodiesel production from waste cooking oil. *J. Mol. Liq.* **2019**, *279*, 224–231. [CrossRef]
75. Ong, H.C.; Mofijur, M.; Silitonga, A.; Gumilang, D.; Kusumo, F.; Mahlia, T. Physicochemical Properties of Biodiesel Synthesised from Grape Seed, Philippine Tung, Kesambi, and Palm Oils. *Energies* **2020**, *13*, 1319. [CrossRef]
76. Silitonga, A.; Masjuki, H.; Mahlia, T.; Ong, H.C.; Kusumo, F.; Aditiya, H.; Ghazali, N. Schleichera oleosa L oil as feedstock for biodiesel production. *Fuel* **2015**, *156*, 63–70. [CrossRef]
77. Aso, A.; Hassan, J.D.S. Investigation of microwave-assisted transesterification reactor of waste cooking oil. *Renew. Energy* **2020**, *162*, 1735–1746. [CrossRef]
78. Mohadesi, M.; Aghel, B.; Maleki, M.; Ansari, A. Production of biodiesel from waste cooking oil using a homogeneous catalyst: Study of semi-industrial pilot of microreactor. *Renew. Energy* **2019**, *136*, 677–682. [CrossRef]
79. Rabelo, S.N.; Ferraz, V.P.; Oliveira, L.S.; Franca, A.S. FTIR Analysis for Quantification of Fatty Acid Methyl Esters in Biodiesel Produced by Microwave-Assisted Transesterification. *Int. J. Environ. Sci. Dev.* **2015**, *6*, 964–969. [CrossRef]
80. Tan, Y.H.; Abdullah, M.O.; Kansedo, J.; Mubarak, N.M.; Chan, Y.S.; Nolasco-Hipolito, C. Biodiesel production from used cooking oil using green solid catalyst derived from calcined fusion waste chicken and fish bones. *Renew. Energy* **2019**, *139*, 696–706. [CrossRef]
81. Bai, H.; Tian, J.; Talifu, D.; Okitsu, K.; Abulizi, A. Process optimisation of esterification for deacidification in waste cooking oil: RSM approach and for biodiesel production assisted with ultrasonic and solvent. *Fuel* **2022**, *318*, 123697. [CrossRef]